



# Ionic strength and pH dependent multi-site sorption of Cs onto a micaceous aquifer sediment <sup>☆</sup>



Adam J. Fuller <sup>a</sup>, Samuel Shaw <sup>b</sup>, Caroline L. Peacock <sup>a</sup>, Divyesh Trivedi <sup>c</sup>, Joe S. Small <sup>c</sup>, Liam G. Abrahamsen <sup>c</sup>, Ian T. Burke <sup>a,\*</sup>

<sup>a</sup> School of Earth and Environment, University of Leeds, Leeds LS2 9JT, UK

<sup>b</sup> School of Earth, Atmospheric and Environmental Sciences, University of Manchester, Manchester M13 9PL, UK

<sup>c</sup> National Nuclear Laboratories, Chadwick House, Warrington Road, Birchwood Park, Warrington WA3 6AE, UK

## ARTICLE INFO

### Article history:

Received 5 August 2013

Accepted 24 October 2013

Available online 1 November 2013

Editorial handling by M. Kersten

## ABSTRACT

Caesium-137 ( $t_{1/2} = 30$  years) is a common contaminant at nuclear legacy sites. Often the mobility of  $^{137}\text{Cs}$  in the environment is governed by its sorption to charged sites within the sediment. To this end it is important to understand the sorption behaviour of caesium across a wide range of environmental conditions. This work investigates the effect of varying solution composition (pH and competing ions) on the sorption of caesium to micaceous aquifer sediment across a large concentration range ( $1.0 \times 10^{-11}$ – $1.0 \times 10^{-1}$  mol L<sup>-1</sup> Cs<sup>+</sup>). Experimental results show that Cs<sup>+</sup> exhibits three distinct sorption behaviours at three different concentration ranges. At very low concentrations  $< 1.0 \times 10^{-6}$  mol L<sup>-1</sup> Cs<sup>+</sup> sorption was unaffected by competition with Na<sup>+</sup> or H<sup>+</sup> but significantly reduced in high ionic strength K<sup>+</sup> solution. Secondly between  $1 \times 10^{-6}$  and  $1.0 \times 10^{-3}$  mol L<sup>-1</sup> Cs<sup>+</sup> is strongly sorbed in a neutral pH, low ionic strength background but sorption is significantly reduced in solutions with either a high concentration of Na<sup>+</sup> or K<sup>+</sup> ions or low pH. At high concentrations  $> 1.0 \times 10^{-3}$  mol L<sup>-1</sup> Cs<sup>+</sup> sorption is reduced in all systems due to saturation of the sediment's sorption capacity. A multi-site cation exchange model was used to interpret the sorption behaviour. From this it was determined that at low concentrations Cs<sup>+</sup> sorbs to the illite frayed edge sites only in competition with K<sup>+</sup> ions. However, once the frayed edge sites are saturated the Cs<sup>+</sup> sorbs to the Type II and Planar sites in competition with K<sup>+</sup>, Na<sup>+</sup> and H<sup>+</sup> ions. Therefore sorption of Cs<sup>+</sup> at concentrations  $> 1.0 \times 10^{-6}$  mol L<sup>-1</sup> is significantly reduced in both high ionic strength and low pH solutions. This is a significant result with regard to predicting the migration of  $^{137}\text{Cs}^+$  in acidic or high ionic strength groundwaters.

© 2013 The Authors. Published by Elsevier Ltd. All rights reserved.

## 1. Introduction

Fallout from nuclear weapons testing and reactor accidents (e.g. Chernobyl, Ukraine; Fukushima, Japan and Three Mile Island, USA) have left many areas of land around the world contaminated with radionuclides (chiefly  $^{137}\text{Cs}^+$ ) (Bandstra et al., 2012; Beresford, 2006). Additionally, legacy wastes from civil power generation are held in storage ponds at a number of nuclear facilities internationally, e.g. Sellafield, UK and Hanford, USA (Babad et al., 1993; McKenzie and Armstrong-Pope, 2010). Accidental and approved releases from these storage facilities have led to contamination of the subsurface (e.g. soils and sediments) and groundwater environments (Chorover et al., 2008; McKenzie and Armstrong-Pope, 2010; Reeve and Eilbeck, 2009). Particular focus has been on the

isotopes of caesium, notably  $^{137}\text{Cs}$  ( $t_{1/2} = 30$  years), which occurs as  $^{137}\text{Cs}^+$  in all environmental situations (Söderlund et al., 2011). As a high yield fission product  $^{137}\text{Cs}^+$  is relatively abundant in nuclear waste (NDA, 2010). It is a high energy gamma emitter, which is not easily shielded by soils and structures (Hill et al., 2001). This makes it one of the main sources of external radiation dose at contaminated sites. Predicting the transport and remediation of Cs<sup>+</sup> contamination at these sites is a major environmental challenge and many studies have reported its environmental behaviour (Beresford, 2006; Livens and Baxter, 1988; Shand et al., 1994). However, developing detailed models of Cs<sup>+</sup> transport requires site specific knowledge of its sorption behaviour, including the effect of changing geochemical conditions (e.g. pH and ionic strength).

It is well established that sorption to clay minerals governs the mobility of Cs<sup>+</sup> in the subsurface environment (Aldaba et al., 2010; Shenber and Eriksson, 1993). Studies into the sorption behaviour of Cs<sup>+</sup> in soils and sediments have traditionally used solution based experimental approaches (mainly batch experiments) to probe these processes (Eberl, 1980; Sawhney, 1972). In soils Cs<sup>+</sup> chiefly sorbs to the surfaces of clay minerals in the fine (<2 μm) fraction

<sup>☆</sup> This is an open-access article distributed under the terms of the Creative Commons Attribution License, which permits unrestricted use, distribution, and reproduction in any medium, provided the original author and source are credited.

\* Corresponding author. Tel.: +44 113 3437532; fax: +44 113 3435259.

E-mail address: [I.T.Burke@leeds.ac.uk](mailto:I.T.Burke@leeds.ac.uk) (I.T. Burke).

(He and Walling, 1996). This is due to their large surface area and high density of charged surface sites (Langmuir, 1997). Like other monovalent cations,  $\text{Cs}^+$  sorbs principally on clay minerals by charge compensating cation exchange (Beresford, 2006; Bouzidi et al., 2010; Cornell, 1993; Hird et al., 1995). Although  $\text{Cs}^+$  will interact with all the charged surfaces in a soil or sediment, it has been shown repeatedly that  $\text{Cs}^+$  sorbs preferentially to some sites before others (de Koning et al., 2007; Francis and Brinkley, 1976; Livens and Loveland, 1988).

$\text{Cs}^+$  selectively sorbs to 2:1 aluminosilicate clays of the mica group, specifically illite ( $\text{K,Ca,Mg}$ )  $(\text{Al,Mg,Fe})_2(\text{Si,Al})_4\text{O}_{10}(\text{OH})_2(\text{H}_2\text{O})$ , through charge compensating cation exchange (Chorover et al., 2008; Cremers et al., 1988; Sawhney, 1972). Illite is a common constituent of many temperate mineral soils (Meunier and Velde, 2004) such as those found at contaminated nuclear sites. Grutter et al. (1986) also noted that Cs can selectively sorb to (illite like) collapsed vermiculate interlayer defects in chlorite. Therefore many studies have focused on the sorption of  $\text{Cs}^+$  to illite or illitic soils and sediments (de Koning et al., 2007; Poinssot et al., 1999; Sawhney, 1972). It is important to be able to accurately predict the likely behaviour of contaminants under all potential circumstances. As sorption of cations is known to be controlled by the ionic strength and pH of the system (Krauskopf and Bird, 1995; Sposito, 1984, 1989) it is important to understand the sorption behaviour of  $\text{Cs}^+$  under a range of geochemical conditions.

Isotherm investigations of  $\text{Cs}^+$  sorption have shown that its uptake onto illitic sediments changes non-linearly with concentration (Campbell and Davies, 1995). Jacobs and Tamura (1960) were the first to propose a multi-site sorption process to account for this non-linearity. They suggested a small number of high affinity sites where  $\text{Cs}^+$  preferentially sorbs, and a large number of non-specific exchange sites. Subsequent authors have used competitive sorption and retention studies to develop this theory. Currently the high affinity sorption sites are thought to be Frayed Edge Sites (FES), which sorb and retain  $\text{Cs}^+$  in preference to other cations (Chorover et al., 2008; Davies and Shaw, 1993; Dyer et al., 2000; Hird et al., 1996). As sorption of  $\text{Cs}^+$  to iron oxides and organic matter is known to be negligible (Campbell and Davies, 1995; Hou et al., 2003), the low affinity sites are commonly assigned to the basal plane of clay minerals. The FES are defined by Nakao et al. (2008) as a partially expanded wedge zone at the edge of the clay interlayer with a basal spacing of 10–14 Å. The FES forms as the mica–illite undergoes weathering of the interlayer which expands from the edge inwards (Jackson, 1968; Jackson et al., 1952).  $\text{Cs}^+$  ions are thought to sorb in this wedge through cation exchange with structural interlayer  $\text{K}^+$  ions at the edge of the particle (Chorover et al., 1999; Kim et al., 1996; Sawhney, 1965). As  $\text{Cs}^+$  is a weakly hydrated cation it is able to readily shed its hydration shell and form inner-sphere complexes with oxygen atoms from the illite tetrahedral layers (Cornell, 1993; Kim et al., 1996; Sawhney, 1972). These sites are inaccessible to more strongly hydrated monovalent and divalent cations (e.g. Na and Ca) so they selectively sorb  $\text{Cs}^+$  from solution (Cremers et al., 1988; de Koning and Comans, 2004; Francis and Brinkley, 1976; Staunton, 1994).

Many authors have tried to use isotherms to elucidate the properties of the FES but the value of this approach is limited because they offer no direct mechanistic explanation for the site or Cs sorption behaviour. However, the introduction of geochemical modelling codes has allowed the complexities of the sorption process to be more effectively explained. A number of different geochemical speciation codes exist including Geochemists workbench (Bethke and Yeakel, 2013), MINSORB (Bradbury and Baeyens, 1997) and PHREEQC (Parkhurst and Appelo, 1999). These vary in both their mathematical formulation of activity coefficients and their programming language and structure. Most investigators have modelled  $\text{Cs}^+$  sorption isotherms for either pure illite systems

(Poinssot et al., 1999) or bulk sediments containing mica/illite (Liu et al., 2004; Steefel et al., 2003; Zachara et al., 2002). The sorption of  $\text{Cs}^+$  in these systems is modelled as a multi-site cation exchange process. Selectivity coefficients ( $K_c$  values) are used to assign one site with high  $\text{Cs}^+$  affinity and one generic site. More recently authors have proposed splitting the high affinity site in two to give a FES and “Type II” sorption site (Bradbury and Baeyens, 2000; Steefel et al., 2003). Experimental evidence for this was obtained by Brouwer et al. (1983) who showed the high affinity site could be divided into a  $\text{Cs}^+$  selective site and a  $\text{Cs}^+/\text{Rb}^+$  selective site. The FES are thought to be located right at the edge of the interlayer, with the Type II site further out in the wedge where the interlayer is slightly expanded (Bradbury and Baeyens, 2000; Brouwer et al., 1983). Although much work has been done on competitive sorption of  $\text{Cs}^+$  in the presence of a variety of other cations (de Koning et al., 2007; Sawhney, 1970) there is limited knowledge of the effect of pH on  $\text{Cs}^+$  uptake by sediments. All previous investigations where pH was varied have been done at trace  $\text{Cs}^+$  concentrations where  $\text{H}^+$  is not expected to compete for the specific FES, and  $\text{Cs}^+$  will be selectively sorbed (Chorover et al., 1999; de Koning et al., 2007; Giannakopoulou et al., 2007). Although it is likely that on the non-specific sites  $\text{H}^+$  will compete with  $\text{Cs}^+$ , this effect has not previously been investigated experimentally. Poinssot et al. (1999) observed some pH dependence at low  $\text{Cs}^+$  concentrations, where sorption to the FES dominates, and they explained this as either mineral dissolution or  $\text{H}^+$  cation exchange.

This study focuses on the Sellafield site, located in West Cumbria, UK on the Irish Sea coast and to the west of the Lake District National Park. The facility is located on heterogeneous glacial drift deposits which overlie a complex succession of Triassic sandstone, Carboniferous limestone and Ordovician volcanics (Chaplow, 1996). The deposits themselves are coarse sediments, with the sand or gravel fraction comprising 90% by weight, and around 1–5% clay sized particles (Randall et al., 2004). The mineralogy is dominated by quartz (65%) and K-feldspar (12%), with the remaining comprised of iron oxides and aluminosilicate clay minerals, dominantly illite (around 70% of the <2  $\mu\text{m}$  fraction) (Dutton et al., 2009; Randall et al., 2004). The site has a complex mix of radioactive and non-radioactive contaminants present as a result of its long history of civil and military nuclear development and waste reprocessing (McKenzie and Armstrong-Pope, 2010). It is reported to be one of the most radioactively contaminated sites in Europe (McKie, 2009) and provides a good test case for understanding the behaviour of radionuclides in the subsurface environment.

This paper presents a study of the sorption behaviour of  $\text{Cs}^+$  at a range of concentrations on a micaceous sediment representative of that underlying the Sellafield site. The first objective of the work was to experimentally describe  $\text{Cs}^+$  sorption across a wide range of  $\text{Cs}^+$  solution concentrations. Batch sorption experiments were used to determine the effect of varying pH and competing ions on the concentration dependent sorption process. This data was then interpreted using a fitted multi-site cation exchange model. The implications of these results for the management of contaminated land at Sellafield are then discussed in detail. However, the results are likely to be broadly applicable to sites with similar mineralogy to Sellafield (especially if illite is present).

## 2. Materials and methods

### 2.1. Sediment collection and storage

Experiments reported here were performed on sediment collected in August 2009 from the Calder Valley, Cumbria. This is close to the Sellafield site, on the same glacial till geological unit as that

underlying the site. After collection, the sediment was oven dried at 40 °C and stored in a HDPE plastic container (Law et al., 2010; Wallace et al., 2012).

## 2.2. Sorption experiments

In this work two types of experiments were performed: concentration variable isotherm experiments where the pH was kept constant and the concentration of Cs<sup>+</sup> varied across a range from  $1.0 \times 10^{-9}$  to  $1.0 \times 10^{-1}$  mol L<sup>-1</sup> and pH sorption edge experiments where a fixed Cs<sup>+</sup> concentration was used, and the pH varied across the range 2–10. Both sets of experiments were conducted using three background solution matrices, namely starting solutions of deionised water (DIW), 1.0 mol L<sup>-1</sup> NaCl and 1.0 mol L<sup>-1</sup> KCl to probe the effect of cationic competition. An initial set of competing ion experiments were performed to determine the most appropriate concentrations of K<sup>+</sup> and Na<sup>+</sup> to use as a background matrix to maximise any competing ion effect. It was determined that both Na<sup>+</sup> and K<sup>+</sup> should be included in the background matrix at a concentration of 1.0 mol L<sup>-1</sup> to ensure an easily measurable competing ion effect was observed (see Supporting information Fig. S1).

The full range of experimental conditions is shown in Table 1, and the specific procedure for setting up each experiment is described below. All experiments were performed in triplicate with a sediment-free control sample to determine if any sorption to the tubes was occurring. Results from the blank experiments showed that there was no sorption of Cs<sup>+</sup> to the tubes under any of the experimental conditions (data not shown). Therefore all Cs<sup>+</sup> sorption was attributed to the sediment.

The solution composition of the system was varied depending on the requirements of the experiment. For all experiments samples of <1.0 mm sieved sediment were pre-wetted with deionised water. Samples were then suspended in the particular experimental solution, containing the desired amount of inactive CsCl, in 50 mL polypropylene Oak Ridge tubes at a solid solution ratio of 100 g L<sup>-1</sup>. Following suspension the samples were spiked with a radiotracer of <sup>137</sup>Cs<sup>+</sup> at a specific activity of 30 Bq mL<sup>-1</sup> (equivalent to  $7.0 \times 10^{-11}$  mol L<sup>-1</sup>). Samples were then agitated for 48 h on an orbital shaker at 140 rpm at room temperature (20 ± 1 °C). Comans et al. (1991) and Poinssot et al. (1999) showed that Cs<sup>+</sup> sorption is kinetically moderated, involving a rapid initial cation exchange process, followed by a period of slow incorporation into the clay structure (Comans and Hockley, 1992). This work focuses solely on the cation exchange process so a 48 h sorption period was chosen to allow pseudo-equilibrium to be reached and for cation exchange processes to reach completion. The pH of the solution

**Table 1**  
Experimental parameters.

Experiment	pH	Initial Cs concentration (mol L <sup>-1</sup> )	Background solution
Isotherms	6.8 ± 0.2	$1 \times 10^{-9}$ mol L <sup>-1</sup> ; $1 \times 10^{-4}$ mol L <sup>-1</sup> ; $1 \times 10^{-1}$ mol L <sup>-1</sup>	Deionised water
			1 mol L <sup>-1</sup> NaCl 1 mol L <sup>-1</sup> KCl
			Deionised water
pH sorption edges	2.0–10.0	$1 \times 10^{-11}$ mol L <sup>-1</sup>	Deionised water
			1 mol L <sup>-1</sup> NaCl 1 mol L <sup>-1</sup> KCl
			$1 \times 10^{-4}$ mol L <sup>-1</sup>
			Deionised water 1 mol L <sup>-1</sup> NaCl 1 mol L <sup>-1</sup> KCl
			$1 \times 10^{-1}$ mol L <sup>-1</sup>
			Deionised water 1 mol L <sup>-1</sup> NaCl 1 mol L <sup>-1</sup> KCl

was measured before and immediately after addition to the sediment and adjusted with 1.0 mol L<sup>-1</sup> HCl and NaOH to overcome the sediments buffering capacity and ensure minimal pH drift during the 48 h equilibration period (when pH was not monitored). Final experimental pH was recorded after 48 h and this value was reported in the results. The pH was recorded using an Orion model 420A bench top pH meter and glass bulb electrode calibrated to pH 4, 7 and 10 using standard buffer solutions. Following the sorption period tubes were centrifuged for 10 min at 6000g. A 1 mL representative sample of the supernatant was then transferred to a liquid scintillation vial containing 10 mL of Ecoscint A solution. Final solution activity (Bq mL<sup>-1</sup>) was then measured by liquid scintillation counting on a Packard Tri-Carb 2100TR liquid scintillation counter with a counting window of 0–280 keV and 10 min counting period. Percentage Cs<sup>+</sup> sorption and distribution coefficient, *K<sub>d</sub>*, values were then calculated using the methodology of Khan et al. (1995) shown in Wallace et al. (2012). The final concentration of other ions (i.e. non-Cs<sup>+</sup>) in the system was not measured.

For the isotherm experiments, the effect of Cs<sup>+</sup> solution concentration on sorption was investigated using CsCl solutions at a range of concentrations between  $1.0 \times 10^{-9}$  mol L<sup>-1</sup> and  $1.0 \times 10^{-1}$  mol L<sup>-1</sup>. Isotherms were performed at circumneutral pH (6.8 ± 0.2); achieved by adjustment with HCl or NaOH (as described above). The sorption behaviour was analysed using a tracer spike of <sup>137</sup>Cs<sup>+</sup> (30 Bq mL<sup>-1</sup> or  $7.0 \times 10^{-11}$  mol L<sup>-1</sup>) and the aqueous activity measured by liquid scintillation counting.

For the pH sorption edge experiments, the effect of pH upon the sorption of Cs<sup>+</sup> was determined by adjusting the initial experimental suspensions with 1.0 mol L<sup>-1</sup> HCl and 1.0 mol L<sup>-1</sup> NaOH to give a pH range from 2 to 10. Samples were pH checked at the beginning of the analysis, and after adjustment to overcome the sediments buffering capacity. The final pH values at the end of a 48 h sorption period are then reported. For the pH experiments three concentrations of Cs<sup>+</sup> were chosen. These were selected based on the different regimes of Cs<sup>+</sup> sorption behaviour displayed in the isotherm experiments and were  $7.0 \times 10^{-11}$  mol L<sup>-1</sup> added as a 30 Bq mL<sup>-1</sup> tracer spike of <sup>137</sup>Cs<sup>+</sup> and  $1.0 \times 10^{-4}$  mol L<sup>-1</sup> and  $1.0 \times 10^{-1}$  mol L<sup>-1</sup> added as CsCl (with a radioactive tracer spike to allow analysis by liquid scintillation counting).

## 2.3. Modelling

A multi-site cation exchange model was constructed in PHREEQCv2 Parkhurst and Appelo (1999) to perform geochemical modelling of Cs<sup>+</sup> sorption to the micaceous sediment. The full PHREEQC modelling input is provided in the Supporting information. The model was based initially on the model of Bradbury and Baeyens (2000). The modelling aim was twofold: Firstly to test the validity of the generic Bradbury and Baeyens (2000) model under scenarios of Cs<sup>+</sup> contamination relevant to Sellafield, and secondly to refine the model in light of our experimental results to provide a specific description and prediction of Cs<sup>+</sup> sorption at Sellafield. The generic *K<sub>c</sub>* values (selectivity coefficients) proposed by Bradbury and Baeyens (2000) for Cs<sup>+</sup> sorption to argillaceous rocks in the presence of competing Na<sup>+</sup> and K<sup>+</sup> ions have been used in previous models of Cs<sup>+</sup> sorption at Sellafield (Randall et al., 2004). These models are used to predict likely sorption and migration of Cs<sup>+</sup> in the subsurface as part of safety case evaluations. Therefore it is extremely important to assess whether the generic Bradbury and Baeyens (2000) model accurately predicts Cs<sup>+</sup> sorption onto Sellafield-like sediments, and to refine the model in light of our experimental investigation to improve the accuracy of future predictive modelling. As experiments were performed across a large ionic strength range the aqueous activity coefficients,  $\gamma$ , were calculated accordingly. At ionic strengths ≤ 0.1 mol L<sup>-1</sup> the extended Debye–Hückel equation was used, with the wateq4f.dat

thermodynamic database (Ball and Nordstrom, 1991). However, in the systems with a total ionic strength  $> 0.1 \text{ mol L}^{-1}$  the Pitzer equations were used, with the Pitzer.dat database (Plummer et al., 1988). A detailed discussion of these calculations is provided in the Supporting information.

#### 2.4. Binary cation exchange

The following section is heavily indebted to Bradbury and Baeyens (2000) whose model this work is based on, and refined from. All the sorption processes within the PHREEQC model are presented as binary cation exchange reactions, according to the Gains–Thomas convention. In the Gains–Thomas approach cation exchange is generically represented as  $m_1\text{-site} + m_2 \leftrightarrow m_2\text{-site} + m_1$ , where  $m_1$  and  $m_2$  are two distinct species (e.g.  $\text{Na}^+$  and  $\text{Cs}^+$ , respectively) and the site is a specific cation exchange site in the sediment. Chemical species exchange in thermodynamic equilibrium with the sorption site, determined by a Gaines and Thomas (1953) mass action equation with an associated equilibrium constant,  $K_c$ . Taking the example of  $\text{Cs}^+$  for  $\text{Na}^+$  exchange this gives  $\frac{K_c}{K_c} = \frac{N_{\text{Cs}}/N_{\text{Na}} \cdot \alpha_{\text{Na}}/\alpha_{\text{Cs}}}{N_m}$  where  $\alpha_i$  is the aqueous activity of the solution species  $i$  and  $N_m$  is the occupancy of the site with the given species,  $m$ , defined by  $N_m = \Gamma_m/Q$  where  $\Gamma$  is the concentration of the sorbed species ( $\text{mol L}^{-1}$ ) on the site and  $Q$  is the total site capacity ( $\text{mol L}^{-1}$ ).

In the model there are several specific sites available for cation exchange and a cation's affinity for each type of site is described by the relevant  $K_c$  value. In the above example, a higher  $K_c$  for any given site indicates that this site has a higher affinity for Cs and would sorb it more readily from solution compared to a site with a lower  $K_c$ . All the  $K_c$  values are normalised against Na (with  $\frac{K_c}{K_c}$  being 1), thus they describe the selectivity of each site for the sorbing ion relative to Na. The  $\frac{K_c}{K_c}$  can be determined from  $\frac{K_c}{K_c}$  and  $\frac{K_c}{K_c}$  using the relationship  $\frac{K_c}{K_c} = \frac{K_c}{K_c} / \frac{K_c}{K_c}$ . In the model,  $K_c$  values are entered as  $\log K_c$ , and are referred to as such throughout.

### 3. Results and discussion

#### 3.1. Sediment characterisation

The sediment was previously characterised by Wallace et al. (2012) and Law et al. (2010), a brief summary is given here. It had a sandy texture containing 94% sand, 5% silt and 1% clay sized particles. Quartz dominated the bulk with minor muscovite, chlorite, albite and microcline also identified by XRD. XRD analysis of the separated clay sized fraction showed it contained quartz, K-feldspar, iron oxides and aluminosilicate clays, namely illite and chlorite (clinochlore). Additionally, SEM observations by Wallace et al. (2012) showed that many of the quartz grains were coated with aluminosilicate clay minerals, suggesting that the surfaces available for reaction within the sediment are likely to be dominated by clay minerals, including illite. Also, Dutton et al. (2009) showed that the same coatings were present on quartz grains in sediment taken from below the Sellafield site. The total cation exchange capacity (CEC) of the sediment, as determined by sorption of copper triethylenetetramine, was  $8.2 \pm 5.1 \text{ meq } 100 \text{ g}^{-1}$  and it had a BET surface area of  $3.4 \pm 0.6 \text{ m}^2 \text{ g}^{-1}$ .

#### 3.2. Cs concentration dependence

To allow maximum clarity for interpretation, the experimental and modelling results are presented in this work in terms of percentage sorption of the initial solution concentration. However, the isotherms (presented in Fig. 1) are also presented in terms of

equilibrium solution and solid concentrations in the Supporting information (Fig. S2).

For those experiments with no competing ion (Fig. 1a) near total sorption of  $\text{Cs}^+$  ( $99.4 \pm 0.2\%$ ) was observed at very low  $\text{Cs}^+$  concentrations ( $1.0 \times 10^{-7} \text{ mol L}^{-1}$ ). This translates to a  $K_d$  of  $1471 \pm 268 \text{ L kg}^{-1}$ . A slight decrease in sorption was determined above this concentration. At  $1 \times 10^{-5} \text{ mol L}^{-1} \text{ Cs}^+$ , sorption was reduced by  $\sim 1\%$  to  $98.4 \pm 0.9\%$  which gives a  $K_d$  of  $695 \pm 373 \text{ L kg}^{-1}$ , a reduction of around 800  $K_d$  units. There was no further significant change in  $\text{Cs}^+$  sorption until  $1.0 \times 10^{-3} \text{ mol L}^{-1}$  where % sorption was reduced to  $93.7 \pm 1.9\%$  with a corresponding  $K_d$  of  $159 \pm 45 \text{ L kg}^{-1}$ . Further reduction in sorption was seen above this  $\text{Cs}^+$  concentration with values of  $46.2 \pm 1.2\%$  at  $1.0 \times 10^{-2} \text{ mol L}^{-1}$  and  $8.3 \pm 6.6\%$  at  $1 \times 10^{-1} \text{ mol L}^{-1}$ . This reflected a reduction in

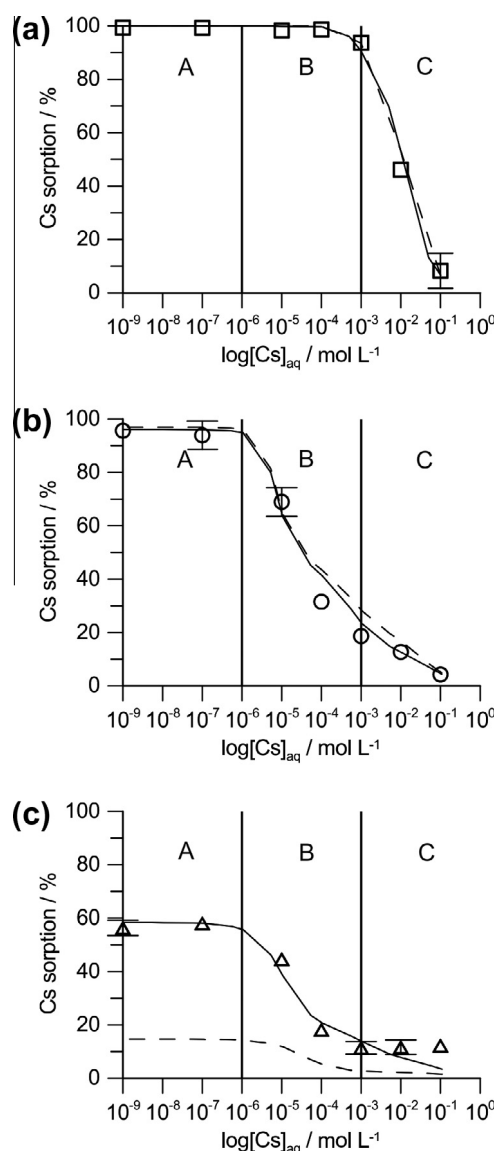


**Fig. 1.** Sorption isotherm showing sorption of  $^{137}\text{Cs}$  ions from a solution of  $\text{CsCl}$  at a range of concentrations; from  $1 \times 10^{-9}$  to  $1 \text{ mol L}^{-1}$  and at a solid solution ratio of  $100 \text{ g L}^{-1}$ . Cs was present in a background of (a) deionised water (b)  $1 \text{ mol L}^{-1} \text{ Na}$  (as  $\text{NaCl}$ ) and (c)  $1 \text{ mol L}^{-1} \text{ K}$  (as  $\text{KCl}$ ). Solid line represents modelling results using the new fitted values. Dotted line represents modelling prediction using generic values from Bradbury and Baeyens (2000). Vertical bars and regions labelled A, B and C differentiate the concentration ranges with different Cs sorption behaviours, see Section 3.2 main text. All data was collected at circumneutral pH. Data points represent the average of a triplicate sample. Error bars are shown on those points where the error (standard deviation) was greater than or equal to the size of the symbol.

sorption of 85.4% over two orders of magnitude of change in  $\text{Cs}^+$  aqueous concentration.

When the concentration dependent sorption experiments were repeated in a background of  $1.0 \text{ mol L}^{-1} \text{ Na}$ , markedly different results were observed (Fig. 1b). Again at the very low concentrations ( $1.0 \times 10^{-7} \text{ mol L}^{-1}$ ) near total Cs sorption occurred ( $95.9 \pm 2.3\%$ , with a  $K_d$  of  $256 \pm 156 \text{ L kg}^{-1}$ ). However, above this concentration there was a reduction in sorption. At  $10^{-5} \text{ mol L}^{-1} \text{ Cs}^+$  only  $71.1 \pm 5.0\%$  ( $K_d$ :  $25 \pm 5 \text{ L kg}^{-1}$ ) of the  $\text{Cs}^+$  is sorbed. This was a reduction of  $\sim 25\%$ , compared to the same concentration of  $\text{Cs}^+$  with no competing ion. There was a steady reduction in percentage sorption as  $\text{Cs}^+$  concentration was increased reaching a minimum value of  $10.8 \pm 1.0\%$  at a  $\text{Cs}^+$  concentration of  $1.0 \times 10^{-1} \text{ mol L}^{-1}$ .

In a background of  $1.0 \text{ mol L}^{-1} \text{ K}^+$  (Fig. 1c) the  $\text{Cs}^+$  sorption behaviour showed a similar trend with maximum sorption between  $1.0 \times 10^{-9}$  and  $1.0 \times 10^{-7} \text{ mol L}^{-1}$ . At  $1.0 \times 10^{-7} \text{ mol L}^{-1}$   $57.3 \pm 1.0\%$  of the  $\text{Cs}^+$  sorbed with a  $K_d$  of  $13 \pm 1 \text{ L kg}^{-1}$ . This then decreased to  $43.7 \pm 0.1\%$  at  $1.0 \times 10^{-5} \text{ mol L}^{-1}$  ( $K_d$   $8 \pm 0 \text{ L kg}^{-1}$ ). A further reduction was then observed at  $1.0 \times 10^{-3} \text{ mol L}^{-1}$  where  $10.0 \pm 2.4\%$  of the  $\text{Cs}^+$  was sorbed. Above an aqueous  $\text{Cs}^+$  concentration of  $1.0 \times 10^{-3} \text{ mol L}^{-1}$  there was no significant reduction in sorption.

Three clear regions are visible within the results (differentiated by solid vertical lines in Fig. 1). At aqueous  $\text{Cs}^+$  concentrations  $< 1.0 \times 10^{-6} \text{ mol L}^{-1}$  (region A) there is near total sorption in the DIW system, and the system with competing  $\text{Na}^+$  ions. However, in the  $\text{K}^+$  competitive system only around 60% of the  $\text{Cs}^+$  sorbs. This is followed by a region (B) of slightly reduced sorption between  $1.0 \times 10^{-6}$  and  $1 \times 10^{-3} \text{ mol L}^{-1}$  in the DIW system. There is a more significant reduction in  $\text{Cs}^+$  sorption in the  $\text{Na}^+$  and in the  $\text{K}^+$  systems. Finally, in the DIW system there is a region (C) of rapidly reduced sorption percentages between  $1.0 \times 10^{-3}$  and  $1.0 \times 10^{-1} \text{ mol L}^{-1}$  above which the sediment reaches sorption saturation. This region of rapidly reducing sorption is also seen in the  $\text{Na}^+$  system, although the total percentage reduction is lower than the DIW system. However, in the  $\text{K}^+$  system the sediment had already reached a minimum sorption by  $1.0 \times 10^{-3} \text{ mol L}^{-1}$  and no further change in sorption was determined at higher  $\text{Cs}^+$  concentrations.

### 3.3. pH dependency

The effect of pH on the sorption of  $\text{Cs}^+$  was investigated at three concentrations of  $\text{Cs}^+$ , chosen to access each of the dominant sorption regions identified from the isotherms. At each of these concentrations 3 distinct pH sorption behaviours were observed as shown in Fig. 2(a–c). At the trace concentrations ( $1.0 \times 10^{-11} \text{ mol L}^{-1}$ ) near total ( $99 \pm 1\%$ ) sorption of  $\text{Cs}^+$  was seen at all pH values. Here the pH had no discernible effect upon the sorption of  $\text{Cs}^+$ . As  $\text{Cs}^+$  concentration was increased, however, to  $1.0 \times 10^{-4} \text{ mol L}^{-1}$  a strong amphoteric effect emerged. A clear sorption edge occurred between pH 2 and 5. At pH 2,  $7.0 \pm 1.5\%$  of the  $\text{Cs}^+$  was sorbed. This increases to  $61.6 \pm 2.9\%$  at pH 3.4 and  $99.3 \pm 0.3\%$  at pH 5.2. Sorption then remained constant as pH was increased before dropping slightly to  $96.9 \pm 1.5\%$  sorption at pH 8.8. Finally, at the saturating concentration of  $1 \times 10^{-1} \text{ mol L}^{-1}$  around 10–15% of the  $\text{Cs}^+$  was sorbed at all pH values and any amphoteric behaviour was masked. Although Poinssot et al. (1999) suggested illite dissolution as a potential cause of reduced  $\text{Cs}^+$  sorption at low pH, they also noted that the rate of dissolution meant that only 0.1% of the illite had dissolved over a 7 day period at pH 3, which is insignificant. The experiments presented here were only run for 48 h so dissolution is likely to be much less than 0.1% of the total illite/clay fraction. Therefore  $\text{H}^+$  competition is most likely the dominant process.

To investigate the interplay between  $\text{H}^+$ ,  $\text{Na}^+$  and  $\text{K}^+$  competition with Cs, pH dependent sorption experiments were also performed

in a background of  $1.0 \text{ mol L}^{-1} \text{ Na}^+$  and  $\text{K}^+$ . Results from pH dependent sorption experiments performed in  $1.0 \text{ mol L}^{-1} \text{ Na}^+$  are shown in Fig. 2d–f. At low concentrations of  $\text{Cs}^+$  ( $1.0 \times 10^{-11} \text{ mol L}^{-1}$  of measured  $^{137}\text{Cs}^+$ , Fig. 2d) near total sorption ( $95 \pm 2\%$ ) of  $\text{Cs}^+$  was determined across the entire pH range with no pH dependency. This is the same as the result for experiments with no competing ions (Fig. 2a). At an elevated concentration ( $1.0 \times 10^{-4} \text{ mol L}^{-1}$ , Fig. 2e) the sorption mainly occurred independently of pH, although a reduction in the sorbed  $\text{Cs}^+$  was measured at pH 2, to  $12.6 \pm 1.1\%$  compared to an average of  $33.0 \pm 7.0\%$  of the  $\text{Cs}^+$  being sorbed across the rest of the pH range (3–10). At highly elevated concentrations of  $\text{Cs}^+$  ( $10^{-1} \text{ mol L}^{-1}$ ) an average of  $17.0 \pm 6.0\%$  of the  $\text{Cs}^+$  was sorbed by the sediment and this process occurred independently of pH, likely due to the higher ratio of  $\text{Cs}^+$  to  $\text{H}^+$  ions.

In the  $\text{K}^+$  dominated system (with  $1.0 \text{ mol L}^{-1} \text{ K}$ , Fig. 2g–i)  $\text{Cs}^+$  sorbed independently of pH at all concentrations. Here at the lowest concentration of  $\text{Cs}^+$  ( $1.0 \times 10^{-11} \text{ mol L}^{-1}$  Fig. 2g) an average of  $37.0 \pm 3.0\%$  of the  $\text{Cs}^+$  was sorbed across the pH range. As the concentration of  $\text{Cs}^+$  was increased to  $1.0 \times 10^{-4} \text{ mol L}^{-1}$  (Fig. 2h) the percentage of  $\text{Cs}^+$  sorbed was reduced to an average of  $11.0 \pm 1.0\%$  across the pH range. Here pH had no effect on  $\text{Cs}^+$  sorption. At the highest  $\text{Cs}^+$  concentration ( $1.0 \times 10^{-1} \text{ mol L}^{-1}$ ) an average of  $19.0 \pm 6.0\%$  of the  $\text{Cs}^+$  was sorbed across the pH range, with no pH effect. This was higher than at  $1.0 \times 10^{-4} \text{ mol L}^{-1}$ ; however, there are large errors on a number of the data points. This is likely due to heterogeneity of the sediment and the extremely high salinity of the system ( $1.0 \text{ mol L}^{-1} \text{ K}^+$  and  $1.0 \times 10^{-1} \text{ mol L}^{-1} \text{ Cs}^+$ ). Again at this high  $\text{Cs}^+$  concentration there was no apparent pH dependency.

### 3.4. Cation exchange modelling

To interpret the sorption behaviour of the  $\text{Cs}^+$  in this system a three site cation exchange model was employed. The model was based on the generic model of Bradbury and Baeyens (2000) and refined as discussed below. In both the Bradbury and Baeyens (2000) model and this refinement of it there are three specific site types for the Cs sorption: Frayed Edge Sites (FES, located right at the edge of the interlayer), Type II sites (located on the edges of the clay particles) and Planar sites (located on the basal plane). Each site is assigned a site concentration (termed site capacity) in  $\text{mol L}^{-1}$  and for each site there is a  $\log K_c$  for the exchange onto the site of  $\text{K}^+$  for  $\text{Na}^+$  ( $\log_{\text{Na}}^{\text{K}} K_c$ ) and  $\text{Cs}^+$  for  $\text{Na}^+$  ( $\log_{\text{Na}}^{\text{Cs}} K_c$ ) (where  $\log_{\text{Na}}^{\text{Na}} K_c$  is 0). Another selectivity constant describing  $\text{H}^+$  exchange for  $\text{Na}^+$  ( $\log_{\text{Na}}^{\text{H}} K_c$ ) was also used in the model. All  $\text{H}^+$  selectivity coefficients (FES, Type II and Planar sites) were initially set to equal 1. In the modelling, site capacities and  $\log K_c$  values were the adjustable parameters used to fit the model to the data.

Initially all the experimental data sets were individually modelled using the generic site capacities for the three sites and  $K_c$  values for  $\text{K}^+$  and  $\text{Cs}^+$  exchange provided by Bradbury and Baeyens (2000). These are listed in Table 2. On inspection of the initial unrefined fits it was determined that both the total estimated CEC and the site ratios were incorrect. Initially the modelling was done using the average CEC value given by Wallace et al. (2012) and the site ratios determined by Bradbury and Baeyens (2000). These were 0.25% FES ( $2.05 \times 10^{-5} \text{ mol L}^{-1}$ ), 20% Type II ( $1.64 \times 10^{-3} \text{ mol L}^{-1}$ ) and 79.75% Planar ( $6.48 \times 10^{-3} \text{ mol L}^{-1}$ ), with a total given CEC of  $8.2 \times 10^{-3} \text{ mol kg}^{-1}$ . The CEC was converted from  $\text{meq } 100 \text{ g}^{-1}$  as measured to  $\text{mol L}^{-1}$ ; as experiments were performed with a solid:solution ratio of 1:10 and Cs is a monovalent ion, this gave a direct conversion of  $1 \text{ meq } 100 \text{ g}^{-1} = 1 \times 10^{-3} \text{ mol L}^{-1}$ . When these site capacities were used it was seen that the Na-competitive isotherm overestimated Cs sorption at all concentrations, but especially at low concentrations (where sorption to the FES and Type II sites dominated). To correct this, the

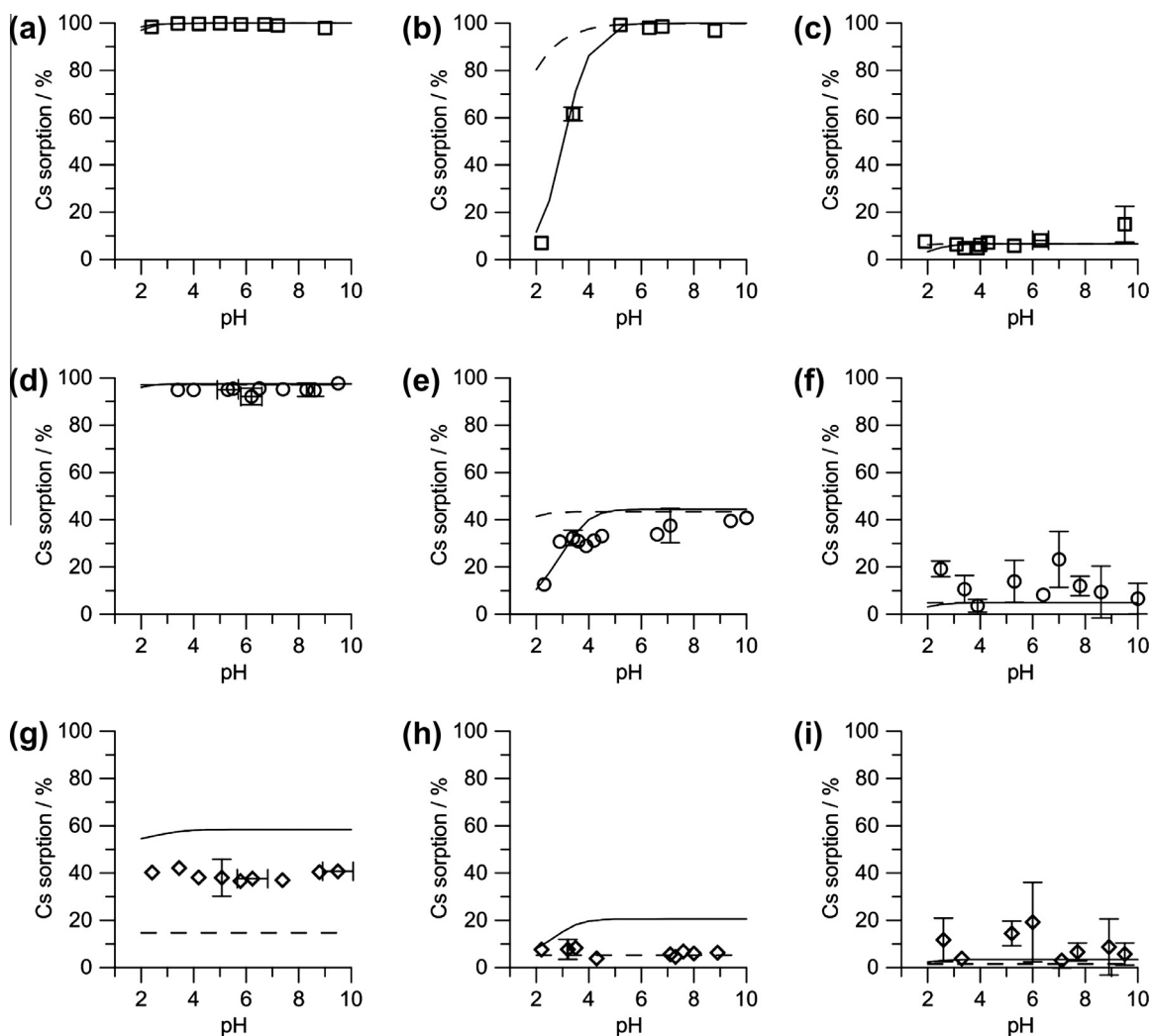


**Fig. 2.** Concentration dependent Cs sorption across a pH range in a background of competing K and Na. Each figure shows a different solution condition: (a)  $10^{-11}$  mol L $^{-1}$  Cs in deionised water; (b)  $10^{-4}$  mol L $^{-1}$  Cs in deionised water; (c)  $10^{-1}$  mol L $^{-1}$  Cs in deionised water; (d)  $10^{-11}$  mol L $^{-1}$  Cs in 1 mol L $^{-1}$  Na; (e)  $10^{-4}$  mol L $^{-1}$  Cs in 1 mol L $^{-1}$  Na; (f)  $10^{-1}$  mol L $^{-1}$  Cs in 1 mol L $^{-1}$  Na; (g)  $10^{-11}$  mol L $^{-1}$  Cs in 1 mol L $^{-1}$  K; (h)  $10^{-4}$  mol L $^{-1}$  Cs in 1 mol L $^{-1}$  K and (i)  $10^{-1}$  mol L $^{-1}$  Cs in 1 mol L $^{-1}$  K. All data points represent averages of triplicate samples. For clarity error bars are not shown where they were smaller than the size of the symbol. Results of modelling using fitted parameters (solid line) and generic parameters from Bradbury and Baeyens (2000) (dashed line) are also shown.

**Table 2**

Modelling exchange  $\log K_c$  values normalised against Na $^+$ .

Source	Exchange species	FES	Type II	Planar
Bradbury and Baeyens (2000)	K $^+$	2.4	2.1	1.1
	Cs $^+$	7.0	3.6	1.6
This paper	K $^+$	1.5	0.6	0.5
	H $^+$	1.8 <sup>a</sup>	3.6	2.5
	Cs $^+$	7.0	3.6	1.6

<sup>a</sup> From Poinssot et al. (1999)

CEC of each site was iteratively adjusted, when keeping all other values constant. This gave new site concentrations of 0.05% FES ( $4.0 \times 10^{-6}$  mol L $^{-1}$ ), 2% Type II ( $1.6 \times 10^{-4}$  mol L $^{-1}$ ) and 97.95% Planar ( $6.5 \times 10^{-3}$  mol L $^{-1}$ ), giving a total CEC of  $6.66 \times 10^{-3}$  mol L $^{-1}$  (which is still within error of the original measured CEC of  $8.2 \pm 5.1 \times 10^{-3}$  mol L $^{-1}$ ). Bradbury and Baeyens (2000) determined their site capacity ratios based on Opalinus clay, which contains around 10% illite. As the sediments used in this study contain a far lower percentage of clay minerals (and therefore less illite), this likely explains the lower concentration of the FES and Type II sites, which are located on the clay minerals.

The sediments also contain comparatively more minerals with planar sites which accounts for the relatively higher percentage of these sites in our system. It should be noted that these new site ratios were close to those used by Steefel et al. (2003) when modelling mixed sediments (rather than a clay rock). The model was then re-run with the new CEC values and the  $\log K_c$  values of Bradbury and Baeyens (2000) and these fits are shown in all figures as dashed lines. From the modelling above it was determined that at all concentrations Cs $^+$  sorption was significantly underestimated in the 1 mol L $^{-1}$  K $^+$  background (dashed line, Fig. 1c). To correct this, the K $^+$  affinity was reduced by iterating the  $\log_{Na}^{K}K_c$  values while maintaining all other values as constant, until a good fit was obtained (solid line Fig. 1c). These new values are shown in Table 2.

From the pH matrix results (Fig. 2), it was found that the model was significantly underestimating the effect of pH at intermediate Cs $^+$  concentrations (dashed lines Fig. 2b and e). Therefore the competitive effect of H $^+$  with Cs $^+$  (represented by  $\log_{Cs}^{H}K_c$  values) was deemed to be too low. The  $\log_{Cs}^{H}K_c$  values were determined by the relationship between the  $\log_{Na}^{H}K_c$  and the  $\log_{Na}^{Cs}K_c$  values as described in Section 2.4. As the  $\log_{Na}^{Cs}K_c$  had previously been fixed in the model adjustment of the  $\log_{Na}^{H}K_c$  was used to increase the

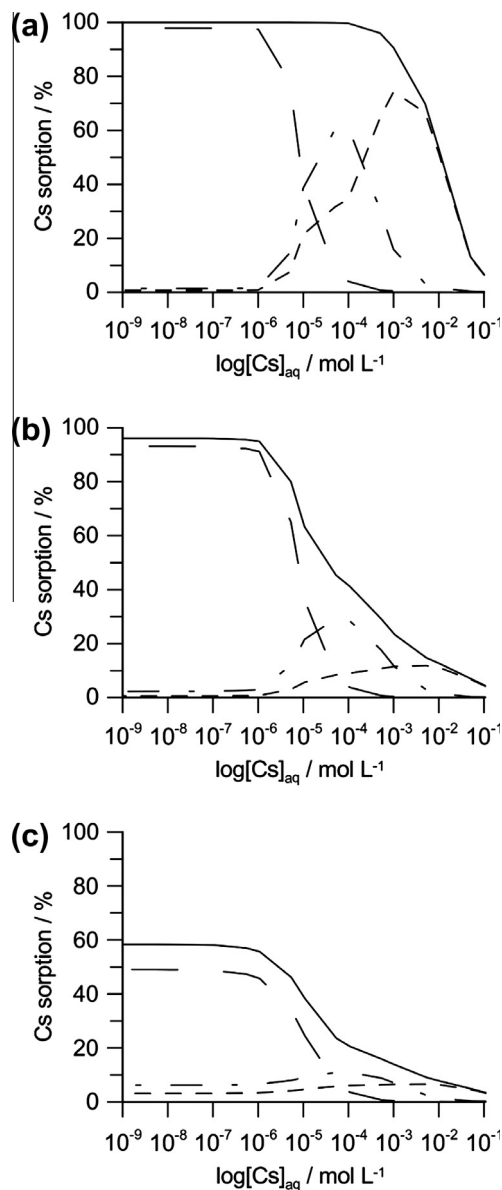


**Fig. 3.** Modelled sorption isotherms showing relative contributions of the three sorption sites (see main text Section 3.4). The long dashed line represents the FES, the dotted and dashed line represents the Type II site and the short dashed line indicates the contributions from the Planar sites. The solid line represents the cumulative total sorption.

modelled pH dependency of Cs sorption in the system and improve the models fit to the experimental data. To do this the  $\log_{\text{Na}}^{\text{H}}K_c$  value for the FES (1.8) was taken from Poinsot et al. (1999). For the Type II and Planar sites no literature values were available. As the focus was on determining the  $\text{Cs}^+/\text{H}^+$  competition of the system the  $\log_{\text{Na}}^{\text{H}}K_c$  values were initially set as equal to  $\log_{\text{Na}}^{\text{Cs}}K_c$  values. As previously, the values were then sequentially iterated until the best fit to the experimental data was obtained. From this it was determined that further refinement of only the planar sites value was required to give a good fit for the pH behaviour seen in the experimental data (Fig. 3). The initial Bradbury and Baeyens (2000) and final adjusted values for all parameters are shown in Table 2 and the final fits are shown as solid lines in all figures. The final model overestimated Cs sorption in the pH varied system with a high K background (Fig. 2g and h). This is an artefact of the fact that  $\log_{\text{Na}}^{\text{K}}K_c$  was refined from the isotherm experiments (Fig. 1c). In that system 60% of the  $\text{Cs}^+$  was sorbed at low concentrations to

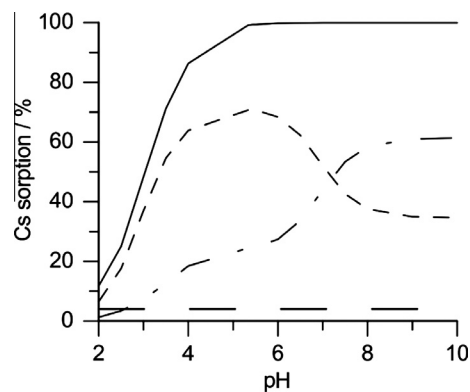


**Fig. 4.** Modelling of  $10^{-4} \text{ mol L}^{-1}$  Cs in a DIW background (see Fig. 3b). Showing relative contribution of the three sorption sites (see Section 3.4 of main text). The long dashed line represents the FES, the dotted and dashed line represents the Type II site and the short dashed line indicates the contributions from the Planar sites. The sum of these three sites, the total sorption, is shown by the solid line.

the FES, at neutral pH. Therefore the model predicts 60% sorption of  $\text{Cs}^+$  across the pH range at low concentrations (Fig. 2g). However, the experimental results presented in Fig. 2g show that only 40% of the  $\text{Cs}^+$  was sorbed at pH 7 (and across the pH range). Therefore the model overestimates  $\text{Cs}^+$  sorption in this system, when compared to the experiment. The difference between % sorption reported from the two experiments is likely due to variation in the illite concentration between the two sub-samples of sediment. At these low concentrations the  $\text{Cs}^+$  would be sorbing to the FES and Type II sites with strong competition from the background  $\text{K}^+$  ions. The relative concentration of these sites in the sediment is extremely low and they are exclusively located on the clay minerals. Therefore a small variation in the total mass of clay minerals (especially illite) between the two sub-samples could give a large variation in the total concentration of FES and Type II sites. In the K rich system a large fraction of these sites would also be occupied by  $\text{K}^+$  rather than  $\text{Cs}^+$  ions. Therefore the effect on total  $\text{Cs}^+$  sorption percentage would be very sensitive to small changes in clay content. This variability between sediment sub-samples is therefore the most likely explanation for the models overestimation of  $\text{Cs}^+$  sorption in Fig. 2g and h. This also presents a major constraint on the accuracy of modelling predictions in environmental scenarios.

It was previously identified from the experimental results (Fig. 1) that there are three regions of distinct  $\text{Cs}^+$  sorption behaviour, governed by the solution concentration. The cation exchange modelling shows that these three sorption regions related to the dominance of the three separate cation exchange sites within the sediment. Fig. 3 shows that at low concentrations, where sorption was only reduced by  $\text{K}^+$  competition,  $\text{Cs}^+$  was sorbed almost exclusively onto the FES. However, when  $\text{Cs}^+$  was present at concentrations above  $10^{-6} \text{ mol L}^{-1}$ , Na effectively reduced  $\text{Cs}^+$  sorption. The model shows that this was due to saturation of the FES and that sorption to the Type II sites dominated, where both  $\text{Na}^+$  and  $\text{K}^+$  could effectively compete with  $\text{Cs}^+$ . Finally above  $10^{-3} \text{ mol L}^{-1}$  Cs, the Planar sites dominated sorption before becoming quickly saturated, which accounts for the reduction in sorption in the DIW system.

Finally, the relative contribution of the different sites to the pH dependent sorption is shown in Fig. 4. This represents the relative contribution of each site for sorption of  $1.0 \times 10^{-4} \text{ mol L}^{-1}$   $\text{Cs}^+$  in a DIW background, which was the system with the strongest pH dependency (experimental data Fig. 2b). Due to the relatively high concentration of  $\text{Cs}^+$  in this system the FES are saturated and contribute to <5% of total sorption. Therefore the Type II and Planar sites control sorption in this system. It can be seen from the results

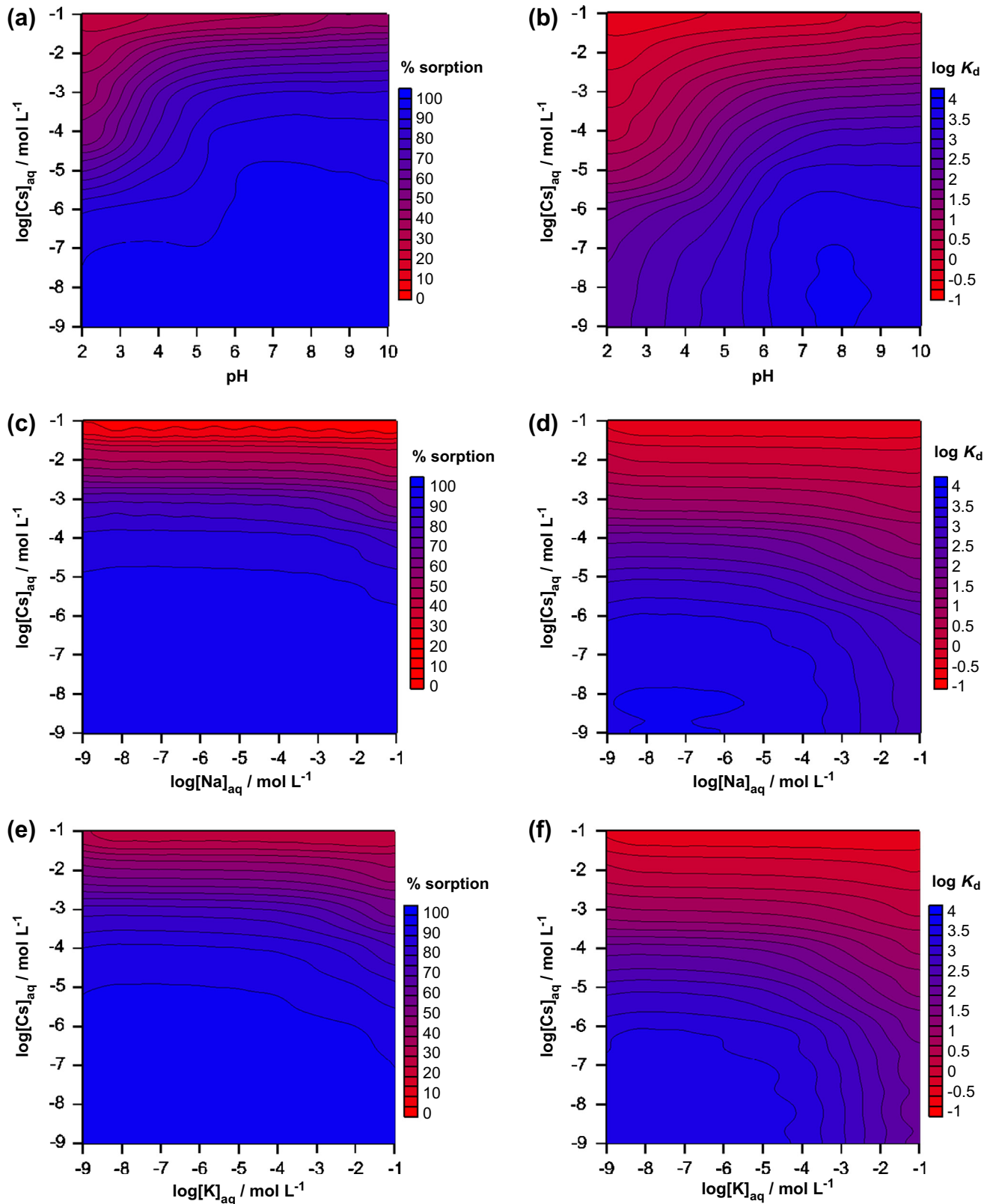


**Fig. 5.** Modelled dependency of Cs sorption on concentrations of H<sup>+</sup>, Na<sup>+</sup> and K<sup>+</sup>. All figures are plotted on log/log axis for clarity. Results are shown in both % sorption and  $\log K_d$  space for ease of reference with blue representing high sorption and red low. (For interpretation of the references to color in this figure legend, the reader is referred to the web version of this article.)

that at low pH the Planar sites dominated the total sorption, however, once the sorption edge reaches its maximum the Type II sites dominate at >pH 7. This was due to the relative balance of the H<sup>+</sup>

and Cs<sup>+</sup>  $K_c$  values of each site (see Table 2). The Type II sites have a higher Cs affinity than the Planar sites, but are far more amphoteric. Therefore at low pH the H<sup>+</sup> out-competed Cs<sup>+</sup> on the Type II



sites and instead the  $\text{Cs}^+$  sorbed to the planar sites, which although they have a lower  $\text{Cs}^+$  affinity also have a low  $\text{H}^+$  affinity. However, at neutral pH and above  $\text{H}^+$  ions cease to affect  $\text{Cs}^+$  sorption and therefore the larger  $\frac{\text{Cs}}{\text{Na}}K_c$  of the Type II sites relative to the Planar sites, means that more  $\text{Cs}^+$  ions sorbed to the Type II sites and it became the dominant control on  $\text{Cs}^+$  sorption, as was seen in the DIW isotherm experiments conducted at neutral pH (Fig. 3a).

### 3.5. Implications for $^{137}\text{Cs}^+$ mobility

The experimental results and modelling outlined in this study have important implications for the potential mobility of  $^{137}\text{Cs}^+$  at contaminated nuclear sites such as Sellafield. It has long been known that a trace amount of  $\text{Cs}^+$  will selectively and irreversibly sorb to the illitic FES (Comans et al., 1991; Cornell, 1993; Hird et al., 1996). However, results presented here show that once the FES are saturated  $\text{Cs}^+$  sorption to the Type II and Planar sites occurs in competition with other cations and is strongly controlled by pH and ionic strength. The current models (e.g. Bradbury and Baeyens (2000)) do not predict the likely impact of  $\text{H}^+$  competition on the sorption of  $\text{Cs}^+$  and greatly overestimate  $\text{Cs}^+$  uptake. The experimental results show during a leak of acidic liquor with high  $\text{Cs}^+$  concentration,  $\text{Cs}^+$  sorption to the sediment will be lower than previously predicted by existing models. Therefore it is recommended that future modelling of this type of scenario at Sellafield use the new selectivity values presented here (Table 2), as they more accurately describe a leak of this nature and may give a more realistic description of likely  $\text{Cs}^+$  migration in acidic liquors. It should be noted however that the modelling results here are calibrated for the experimental conditions, specifically the sediment particle size and experiment solid: solution ratio. In applying the new model to site specific reactive transport scenarios it is important to account for variation in these parameters. Hydrological parameters such as sediment density and porosity should also be considered. This paper presents a simple cation exchange model, rather than a reactive transport model so these hydrological factors are not considered.

The fact that  $\text{H}^+$  competes with  $\text{Cs}^+$  for the Type II and Planar sites is an important new finding with implications for management and modelling of  $\text{Cs}^+$  sorption and migration from acidic leaks. However, the results also show that in alkaline leaks, which are much more common at Sellafield (Wallace et al., 2012; Thorpe et al., 2012), all the  $\text{Cs}^+$  present will sorb to the clay fraction, even if the FES are saturated. It should also be noted that the ability of  $\text{K}^+$  and  $\text{Na}^+$  to compete with  $\text{Cs}^+$  is an important controlling factor on  $\text{Cs}^+$  sorption potential. These results have shown that at high concentrations ( $1.0 \text{ mol L}^{-1}$ )  $\text{K}^+$  can significantly reduce sorption of  $\text{Cs}^+$  to the FES. Where the FES is saturated both  $\text{Na}^+$  and  $\text{K}^+$  can also significantly reduce the sorption of  $\text{Cs}^+$  to the less specific Planar and Type II sites. This is especially noticeable in the high ionic strength solutions tested here. Therefore in highly alkaline liquors, rich in  $\text{NaOH}$  and  $\text{KOH}$  (such as young cement leachates), or salty solutions, rich in  $\text{NaCl}$  and  $\text{KCl}$  (such as seawater),  $\text{Cs}^+$  sorption may be significantly reduced by cationic competition.

To summarise all of the findings of this work the refined cation exchange model was used to predict the sorption of  $\text{Cs}^+$  under a wide range of solution conditions and contour plots were constructed (Fig. 5). The concentration of  $\text{Cs}^+$  is the most important parameter controlling its sorption behaviour. Therefore the effect of pH,  $\text{Na}^+$  and  $\text{K}^+$  concentrations were modelled with relation to increasing  $\text{Cs}^+$  concentration. These results are expressed in both  $K_d$  and % sorption terms for ease of reference. The results of this modelling clearly show that  $\text{Cs}^+$  sorption is governed by the concentration of different ions in solution, as previously described. The system where pH was varied (Fig. 5a and b) shows two regions where pH has little effect on sorption. More than 90% of the  $\text{Cs}^+$

sorbs across the whole pH range at very low  $\text{Cs}^+$  concentrations ( $<1.0 \times 10^{-7} \text{ mol L}^{-1}$ ). Sorption is also pH independent at very high  $\text{Cs}^+$  concentrations ( $>1.0 \times 10^{-2} \text{ mol L}^{-1}$ ), however  $<10\%$  of the  $\text{Cs}^+$  sorbs. The pH of the system has the greatest effect at intermediate  $\text{Cs}^+$  concentrations, with a clear sorption edge between pH 3 and 5 most visible at  $\text{Cs}^+$  concentrations between  $1.0 \times 10^{-2}$  and  $1.0 \times 10^{-6} \text{ mol L}^{-1}$ .  $\text{Na}^+$  has a less clear impact of  $\text{Cs}^+$  sorption than pH. Fig. 5c and d shows that  $\text{Cs}^+$  sorption in the  $\text{Na}^+$  background system is largely governed by the  $\text{Cs}^+$  concentration (and therefore saturation of the sediments CEC). When expressed in  $K_d$  terms (Fig. 5d) it is clearer that when  $\text{Na}^+$  is present at concentrations  $>1.0 \times 10^{-3} \text{ mol L}^{-1}$  it competes with  $\text{Cs}^+$  and reduces total sorption. This is most noticeable at  $\text{Cs}^+$  concentration between  $1.0 \times 10^{-6}$  and  $1.0 \times 10^{-3} \text{ mol L}^{-1}$ . Finally  $\text{K}^+$  effectively competes with  $\text{Cs}^+$  at all concentrations when present at concentrations  $>1.0 \times 10^{-4} \text{ mol L}^{-1}$  (Fig. 5e and f). This competition effect is masked above  $\text{Cs}^+$  concentration of  $10^{-2} \text{ mol L}^{-1}$  where the sediments sorption capacity is saturated and  $<10\%$  of the total  $\text{Cs}^+$  sorbs. These modelling outputs give a strong prediction of likely  $\text{Cs}^+$  sorption under a wide range of measureable conditions. Therefore it is essential when predicting the potential mobility of  $\text{Cs}^+$  from leaks at Sellafield, and other nuclear sites, with similar near surface mineralogy (illite present), that the groundwater conditions and the chemistry of the leak solution are known.

The Nuclear Decommissioning Authority's inventory of waste at Sellafield (NDA, 2007; SellafieldLtd, 2009) shows that  $\text{Cs}^+$  is present at high concentrations in a number of wastes on the sites. Notably at around  $1 \times 10^{-5} \text{ mol L}^{-1}$  in both the Magnox cladding waste and Magnox fuel pond sludge, which are known to have leaked to ground (McKenzie et al., 2011; Wallace et al., 2012). Other high level liquid wastes contain up to  $2 \times 10^{-2} \text{ mol L}^{-1}$  of  $\text{Cs}^+$  (NDA, 2007; leaks from this source are currently not reported or suspected), which is in the sorption regime where both the FES and Type II sites would be saturated. Therefore this new modelling predicts that if the wastes containing  $\text{Cs}^+$  at these very high concentrations were to leak then sorption is likely to be significantly reduced in groundwater with either low pH (e.g. an acid leak) or high ionic strength (e.g. seawater intrusion). However, they also show that the  $\text{Cs}^+$  could be effectively immobilised by either buffering the pH of the system to  $>\text{pH } 5$  or reducing the ionic strength. Therefore it is important that any  $\text{Cs}^+$  bearing solutions are treated to neutralise their pH and reduce their ionic strength.

## 4. Conclusion

Here it has been shown through experimentation and cation exchange modelling that  $\text{Cs}^+$  sorption to a micaceous aquifer sediment representative of those at the Sellafield site was predominantly controlled by  $\text{Cs}^+$  solution concentration. At intermediate and high  $\text{Cs}^+$  solution concentrations ( $>10^{-6} \text{ mol L}^{-1}$ ) the pH and ionic strength of the system are of great importance due to the multi-site nature of the  $\text{Cs}^+$  sorption to these sediments. The Frayed Edge Sites (FES) selectively sorb  $\text{Cs}^+$  in preference to other solution cations, but are quickly saturated. Once they become saturated, excess  $\text{Cs}^+$  sorbs to the non-specific Type II and Planar sites where other cations can effectively compete and reduce total  $\text{Cs}^+$  sorption. Under most leak scenario conditions  $\text{Cs}^+$  concentrations would be low enough that the FES are far from saturation. Therefore in these circumstances most of the  $\text{Cs}^+$  will sorb to the FES regardless of solution conditions. However, under the scenario of an acidic leak with high  $\text{Cs}^+$  concentrations present, a significant amount of the  $\text{Cs}^+$  may migrate further than predicted by existing models because these do not account for  $\text{H}^+$  competition.

## Acknowledgements

Thanks are offered to Sarah Wallace for sharing knowledge of the sediment and advice on experimental procedures. This work was funded by the UK Engineering and Physical Sciences Research Council industrial CASE Studentship #10000173 in partnership with National Nuclear Laboratory Ltd. awarded to AJF.

## Appendix A. Supplementary material

Supplementary data associated with this article can be found, in the online version, at <http://dx.doi.org/10.1016/j.apgeochem.2013.10.017>.

## References

- Aldaba, D., Rigol, A., Vidal, M., 2010. Diffusion experiments for estimating radiocesium and radiostromium sorption in unsaturated soils from Spain: comparison with batch sorption data. *J. Hazard. Mater.* 181, 1072–1079.
- Babad, H., Cash, R.J., Deichman, J.L., Johnson, G.D., 1993. High-priority Hanford site radioactive waste storage tank safety issues: an overview. *J. Hazard. Mater.* 35, 427–441.
- Ball, J.W., Nordstrom, D.K., 1991. User's manual for WATEQ4F with revised thermodynamic database and test cases for calculating speciation of major, trace and redox elements in natural waters. Open-File Report 91–183. USGS, Denver.
- Bandstra, M.S., Vetter, K., Chivers, D.H., Aucott, T., Bates, C., Coffey, A., Curtis, J., Hogan, D., Iyengar, A., Looker, Q., Miller, J., Negut, V., Plimley, B., Satterlee, N., Supic, L., Yee, B., 2012. Measurements of Fukushima fallout by the Berkeley radiological air and water monitoring project. In: Nuclear Science Symposium and Medical Imaging Conference (NSS/MIC), pp. 18–24.
- Beresford, N.A., 2006. Land contaminated by radioactive materials. *Soil Use Manage.* 21, 468–474.
- Bethke, C.M., Yeakel, S., 2013. The Geochemists Workbench: Reference Manual.
- Bouzidi, A., Souahri, F., Hanini, S., 2010. Sorption behavior of cesium on Ain Oussera soil under different physicochemical conditions. *J. Hazard. Mater.* 184, 640–646.
- Bradbury, M.H., Baeyens, B., 1997. A mechanistic description of Ni and Zn sorption on Na-montmorillonite Part II: modelling. *J. Contam. Hydrol.* 27, 223–248.
- Bradbury, M.H., Baeyens, B., 2000. A generalised sorption model for the concentration dependent uptake of caesium by argillaceous rocks. *J. Contam. Hydrol.* 42, 141–163.
- Brouwer, E., Baeyens, B., Maes, A., Cremers, A., 1983. Cesium and rubidium ion equilibrium in illite clay. *J. Phys. Chem.* 87, 1213–1219.
- Campbell, L.S., Davies, B.E., 1995. Soil sorption of caesium modelled by the Langmuir and Freundlich isotherm equations. *Appl. Geochem.* 10, 715–723.
- Chaplow, R., 1996. The geology and hydrogeology of Sellafield: an overview. *Quart. J. Eng. Geol.* 29, S1–S12.
- Chorover, J., Choi, S., Rotenberg, P., Serne, R.J., Rivera, N., Strepka, C., Thompson, A., Mueller, K.T., O'Day, P.A., 2008. Silicon control of strontium and cesium partitioning in hydroxide-weathered sediments. *Geochim. Cosmochim. Acta* 72, 2024–2047.
- Chorover, J., DiChiaro, M.J., Chadwick, O.A., 1999. Structural charge and cesium retention in a chronosequence of tephritic soils. *Soil Sci. Soc. Am. J.* 63, 169–177.
- Comans, R.N.J., Haller, M., Depreter, P., 1991. Sorption of cesium on illite: none-equilibrium behaviour and reversibility. *Geochim. Cosmochim. Acta* 55, 433–440.
- Comans, R.N.J., Hockley, D.E., 1992. Kinetics of cesium sorption on illite. *Geochim. Cosmochim. Acta* 56, 1157–1164.
- Cornell, R., 1993. Adsorption of cesium on minerals: a review. *J. Radioanal. Nucl. Chem.* 171, 483–500.
- Cremers, A., Elsen, A., Depreter, P., Maes, A., 1988. Quantitative analysis of radiocaesium retention in soils. *Nature* 335, 247–249.
- Davies, K.S., Shaw, G., 1993. Fixation of Cs-137 by soils in sediments in the Esk Estuary, Cumbria, UK. *Sci. Total Environ.* 132, 71–92.
- de Koning, A., Comans, R.N.J., 2004. Reversibility of radiocaesium sorption on illite. *Geochim. Cosmochim. Acta* 68, 2815–2823.
- de Koning, A., Konoplev, A.V., Comans, R.N.J., 2007. Measuring the specific caesium sorption capacity of soils, sediments and clay minerals. *Appl. Geochem.* 22, 219–229.
- Dutton, M.V., Foster, C., Trivedi, D., 2009. Characterisation of Soils from B38 Site Investigation within the Sellafield Separation Area. NNL Commercial.
- Dyer, A., Chow, J.K.K., Umar, I.M., 2000. The uptake of caesium and strontium radioisotopes onto clays. *J. Mater. Chem.* 10, 2734–2740.
- Eberl, D.D., 1980. Alkali cation selectivity and fixation by clay minerals. *Clay Clay Miner.* 28, 161–172.
- Francis, C.W., Brinkley, F.S., 1976. Preferential adsorption of <sup>137</sup>Cs to micaceous minerals in contaminated freshwater sediment. *Nature* 260, 511–513.
- Gaines, G.L., Thomas, H.C., 1953. Adsorption studies on clay minerals 2: a formulation of the thermodynamics of exchange adsorption. *J. Chem. Phys.* 21, 714–718.
- Giannakopoulou, F., Haidouti, C., Chronopoulou, A., Gasparatos, D., 2007. Sorption behavior of cesium on various soils under different pH levels. *J. Hazard. Mater.* 149, 553–556.
- Grutter, A., Von Gunten, H.R., Rossler, E., 1986. Sorption, desorption, and isotope exchange of cesium ( $10^{-9}$ – $10^{-3}$  M) on chlorite. *Clays Clay Miner.* 34, 677–680.
- He, Q., Walling, D.E., 1996. Interpreting particle size effects in the adsorption of Cs-137 and unsupported Pb-210 by mineral soils and sediments. *J. Environ. Radioact.* 30, 117–137.
- Hill, M.D., Steeds, J.E., Slade, N.J., 2001. Land Contamination: Technical Guidance on Special Sites: Nuclear Sites. Environment Agency, Bristol.
- Hird, A.B., Rimmer, D.L., Livens, F.R., 1995. Total caesium-fixing potentials of acid organic soils. *J. Environ. Radioact.* 26, 103–118.
- Hird, A.B., Rimmer, D.L., Livens, F.R., 1996. Factors affecting the sorption and fixation of caesium in acid organic soil. *Eur. J. Soil Sci.* 47, 97–104.
- Hou, X.L., Fogh, C.L., Kucera, J., Andersson, K.G., Dahlgard, H., Nielsen, S.P., 2003. Iodine-129 and caesium-137 in Chernobyl contaminated soil and their chemical fractionation. *Sci. Total Environ.* 308, 97–109.
- Jackson, M.L., 1968. Weathering of primary and secondary minerals in soils. In: 9th International Congress of Soil Science. The International Society of Soil Science and Angus & Robertson Ltd., Adelaide, Australia, pp. 281–292.
- Jackson, M.L., Hseung, Y., Corey, R.B., Evans, E.J., Heuvel, R.C.V., 1952. Weathering sequence of clay-size minerals in soils and sediments: II. Chemical weathering of layer silicates. *Soil Sci. Soc. Am. Proc.* 16, 3–6.
- Jacobs, D.G., Tamura, T., 1960. The mechanism of ion fixation using radio-isotope techniques. In: 7th International Congress of Soil Science. The International Society of Soil Science, Madison, Wisconsin, USA, pp. 206–214.
- Khan, S.A., Riazur, Rehman, Khan, M.A., 1995. Sorption of strontium on bentonite. *Waste Manage. (Oxford)* 15, 641–650.
- Kim, Y., Kirkpatrick, R.J., Cygan, R.T., 1996. Cs-133 NMR study of cesium on the surfaces of kaolinite and illite. *Geochim. Cosmochim. Acta* 60, 4059–4074.
- Krauskopf, K.B., Bird, D.K., 1995. Introduction to Geochemistry, third ed. McGraw-Hill, New York.
- Langmuir, D., 1997. Aqueous Environmental Geochemistry. Prentice Hall, New Jersey.
- Law, G.T.W., Geissler, A., Boothman, C., Burke, I.T., Livens, F.R., Lloyd, J.R., Morris, K., 2010. Role of nitrate in conditioning aquifer sediments for technetium bioreduction. *Environ. Sci. Technol.* 44, 150–155.
- Liu, C.X., Zachara, J.M., Smith, S.C., 2004. A cation exchange model to describe Cs+ sorption at high ionic strength in subsurface sediments at Hanford site, USA. *J. Contam. Hydrol.* 68, 217–238.
- Livens, F.R., Baxter, M.S., 1988. Chemical associations of artificial radionuclides in Cumbrian soils. *J. Environ. Radioact.* 7, 75–86.
- Livens, F.R., Loveland, P.J., 1988. The influence of soil properties on the environmental mobility of caesium in Cumbria. *Soil Use Manage.* 4, 69–75.
- McKenzie, H., Armstrong-Pope, N., 2010. Groundwater Annual Report 2010. Sellafield Ltd.
- McKenzie, H.M., Coughlin, D., Laws, F.A.S., 2011. Groundwater Annual Report 2011. Sellafield Ltd.
- McKie, R., 2009. Sellafield: The Most Hazardous Place in Europe. <<http://www.theguardian.com/environment/2009/apr/19/sellafield-nuclear-plant-cumbria-hazards>> (accessed 31.07.13).
- Meunier, A., Velde, V., 2004. Illite. Springer-Verlag, Berlin.
- Nakao, A., Thiry, Y., Funakawa, S., Kosaki, T., 2008. Characterization of the frayed edge site of micaceous minerals in soil clays influenced by different pedogenetic conditions in Japan and northern Thailand. *Soil Science & Plant Nutrition* 54, 479–489.
- NDA, 2007. Sellafield High Level Liquid Waste Inventory 2D02.
- NDA, 2010. The 2010 UK Radioactive Waste Inventory.
- Parkhurst, D.L., Appelo, C.A.J., 1999. User's Guide to PHREEQC (Version 2). US Geological Survey, Denver.
- Plummer, L.N., Parkhurst, D.L., Fleming, G.W., Dunkle, S.A., 1988. A Computer Program Incorporating Pitzer's Equation for Calculation of Geochemical Reactions in Brines. Water-Resources Investigations Report, 88–4153. USGS, Virginia.
- Poinssot, C., Baeyens, B., Bradbury, M.H., 1999. Experimental and modelling studies of caesium sorption on illite. *Geochim. Cosmochim. Acta* 63, 3217–3227.
- Randall, M.G., Brydie, J., Graham, J., Small, J.S., 2004. SCLS Phase 1: The Geochemistry of the Sellafield Site. BNFL Commercial.
- Reeve, P., Eilbeck, K., 2009. Contaminated land and groundwater management at Sellafield, a large operational site with significant legacy and contaminated land challenges. In: 11th International Conference on Environmental Remediation and Radioactive Waste Management, ICEM'07, September 2, 2007–September 6, 2007, PART A ed. American Society of Mechanical Engineers, Bruges, Belgium, pp. 431–437.
- Sawhney, B.L., 1965. Sorption of cesium from dilute solutions. *Soil Sci. Soc. Am. Proc.* 29, 25–28.
- Sawhney, B.L., 1970. Potassium and cesium ion selectivity in relation to clay mineral structure. *Clay Clay Miner.* 18, 47–&.
- Sawhney, B.L., 1972. Selective sorption and fixation of cations by clay-minerals – review. *Clay Clay Miner.* 20, 93–100.
- SellafieldLtd, 2009. Generic Basics for Inventory Challenge – Legacy Alkaline Sludge Systems. Sellafield Ltd., Cumbria, UK.
- Shand, C.A., Cheshire, M.V., Smith, S., Vidal, M., Rauret, G., 1994. Distribution of radiocesium in organic soils. *J. Environ. Radioact.* 23, 285–302.
- Shenber, M.A., Eriksson, A., 1993. Sorption behavior of cesium in various soils. *J. Environ. Radioact.* 19, 41–51.

- Söderlund, M., Lusa, M., Lehto, J., Hakanen, M., Vaaramaa, K., Lahdenperä, A.-M., 2011. Sorption of Iodine, Chlorine, Technetium, and Cesium in Soil. Posiva, Eurajoki, Finland.
- Sposito, G., 1984. *The Surface Chemistry of Soils*. Oxford University Press, New York.
- Sposito, G., 1989. *The Chemistry of Soils*. Oxford University Press, New York.
- Staunton, S., 1994. Adsorption of radiocaesium on various soils: interpretation and consequences of the effects of soil: solution ratio and solution composition on the distribution coefficient. *Eur. J. Soil Sci.* 45, 409–418.
- Steeffel, C.L., Carroll, S., Zhao, P., Roberts, S., 2003. Cesium migration in Hanford sediment: a multisite cation exchange model based on laboratory transport experiments. *J. Contam. Hydrol.* 67, 219–246.
- Thorpe, C.L., Law, G.T.W., Boothman, C., Lloyd, J.R., Burke, I.T., Morris, K., 2012. The synergistic effects of high nitrate concentrations on sediment bioreduction. *Geomicrobiol. J.* 29, 484–493.
- Wallace, S.H., Shaw, S., Morris, K., Small, J.S., Fuller, A.J., Burke, I.T., 2012. Effect of groundwater pH and ionic strength on strontium sorption in aquifer sediments: implications for <sup>90</sup>Sr mobility at contaminated nuclear sites. *Appl. Geochem.* 27, 1482–1491.
- Zachara, J.M., Smith, S.C., Liu, C.X., McKinley, J.P., Serne, R.J., Gassman, P.L., 2002. Sorption of Cs+ to micaceous subsurface sediments from the Hanford site, USA. *Geochim. Cosmochim. Acta* 66, 193–211.